Available online at http://jprm.sms.edu.pk/
Journal of Prime Research in Mathematics, (2026), 191–202

Journal of Prime Research in Mathematics

Comparative Study of Fractional and Integer-Order Telegraph Equations: Numerical Methods and Stability Analysis

Mahmut Modanli[a], Fatih Ozbag[a,*]

[a] *Department of Mathematics, Harran University, Sanliurfa, 63300, Turkey.*

Abstract

This study investigates the numerical solutions of the time-fractional telegraph equation formulated using the Caputo derivative. Employing both first-order and second-order finite difference schemes, we establish stable discretization methods to approximate the solution of the equation. Theoretical stability analyses are presented for each scheme. To assess the accuracy and performance of the methods, we conduct numerical experiments comparing the results of the fractional-order model with those of the classical integer-order case. The comparison demonstrates that the second-order scheme yields superior accuracy over the first-order scheme, and that the fractional-order formulation offers improved approximations compared to its classical counterpart. The analytical and numerical solutions are graphically illustrated using MATLAB, confirming the reliability and efficiency of the proposed methods.

Keywords: Time-fractional telegraph equation, Caputo derivative, finite difference method, numerical stability, accuracy comparison.

2010 Mathematics Subject Classification: 65M06, 65M12, 35R11

1. Introduction

Partial differential equations (PDEs) have numerous applications in sciences such as electrodynamics, hydrodynamics, electromagnetism, thermodynamics, fluid dynamics, elasticity, materials science and wave propagation [8, 30, 27]. Many studies have been done on classical and fractional order partial differential equations. Fractional calculus is defined as the study of non-integer order integral and differential operators. Models using fractional order differential operators have been discovered to have a significant role in explaining physical occurrences, and fractional differential evolution models are more precise and efficient than previously employed in classical models. [4, 27, 29, 16, 33, 22]. A wide range of disciplines, such as biology, engineering, seismology, and finance, have studied the benefits of fractional derivative operators

*Corresponding author
Email addresses: mmodanli@harran.edu.tr (Mahmut Modanli), fozbag@harran.edu.tr (Fatih Ozbag)

Received : 20 October 2026*; Accepted:* 05 May 2026*; Published Online:* 20 June 2026

[13, 20, 12, 24].The analytical and approximative solutions of fractional order equations have been obtained via the use of several effective and potent approaches. Some of these techniques are; Elzaki transform method [21], theta-method [19], a wavelet operational method [31], homotopy perturbation Sumudu transform method [28], a hybrid interpolation method [9], fractional Laplace differential transform method [25], new two step Laplace Adam-Bashforth method [7], Laplace Adomian decomposition method [15], a unified Petrov–Galerkin spectral method [34], Crank–Nicholson finite difference method [1], the combined Shooting-Pseudo-Arclength method [17], modified double conformable Laplace transform method [23], the Laplace optimized decomposition method [5], new iterative method [32], and a novel approach, called (MHB-DQM) in [10].

The telegraph equation, which describes signal propagation with finite speed in transmission lines, has long been studied in mathematical physics and engineering [18, 11]. It models wave-like phenomena with damping effects and appears in various fields including electrical engineering, viscoelasticity, and heat conduction [14]. Traditional integer-order models often fall short in accurately capturing memory and hereditary properties of complex media. In response, fractional-order generalizations especially those involving Caputo derivatives have gained attention for their improved realism in modeling such systems. Despite the growing body of research on fractional telegraph equations, many existing studies rely on analytical or semi-analytical methods, with relatively limited work focusing on robust numerical schemes [6, 3]. The novelty of this research lies in developing and analyzing both first- and second-order finite difference methods for the time-fractional telegraph equation with dual Caputo derivatives, providing stability proofs and conducting a detailed accuracy comparison with the classical model. This dual-level comparison offers new insights into the performance benefits of fractional modeling and the effectiveness of higher-order numerical schemes.

Now, we shall give some basic definitions about fractional derivates and then introduce the studied problem.

Definition 1.1. The definition of the gamma function is

$$\Gamma(z) = \int_0^\infty e^{-t} t^{z-1} dt, \text{ for all } z \neq 0, -1, -2, ... \in C. \tag{1.1}$$

Definition 1.2. $D_\xi^\alpha y(\xi, x)$ is called α order time fractional Caputo derivative and defined by

$$\frac{\partial^\alpha y(\xi, x)}{\partial \xi^\alpha} = D_\xi^\alpha y(\xi, x) = \frac{1}{\Gamma(n-\alpha)} \int_0^\xi \frac{1}{(\xi - p)^{\alpha - n + 1}} \frac{\partial^n y(p, x)}{\partial p^n} dp, \quad (n - 1 < \alpha < n)$$

and for $\alpha = n \in N$ defined by:

$$D_\xi^\alpha y(\xi, x) = \frac{\partial^\alpha y(\xi, x)}{\partial \xi^\alpha} = \frac{\partial^n y(\xi, x)}{\partial \xi^n}.$$

In this work, we consider following time fractional order telegraph partial differential equation

$$\begin{cases} {}_0^C D_\xi^\beta y(\xi, x) + {}_0^C D_\xi^\alpha y(\xi, x) + \lambda y(\xi, x) = y_{xx}(\xi, x) + f(\xi, x), \\ 0 < \xi < T, \ 0 < x < l, \\ y(0, x) = v_0(x), \ y_\xi(0, x) = v_1(x), \ 0 \le x \le l, \\ y(\xi, 0) = y(\xi, l) = 0, \ 0 \le \xi \le T, \\ 1 < \beta \le 2, \ 0 < \alpha \le 1 \end{cases} \tag{1.2}$$

where $v_0(x), v_1(x)$ and $f(\xi, x)$ are the smooth functions for $x \in (0, l)$ and $\xi \in (0, T)$, and $y(\xi, x)$ is the solution of time fractional order pde (1.2). ${}_0^C D_\xi^\beta y(\xi, x)$ is β order Caputo derivative and ${}_0^C D_\xi^\alpha y(\xi, x)$ is α order Caputo derivative.

For the rest of the paper, we give the abstract form of the problem and its solution, stability analysis and a numerical test example to confirm the theoretical statements.

2. Abstract form and solution of the problem

In the $H = L_2$ space defined on $[0, l]$, using the method [2], we can write the problem (1.2) as the following abstract ordinary differential equation form

$$\begin{cases} {}_0^C D_\xi^\beta y(\xi) + {}_0^C D_\xi^\alpha y(\xi) + P y(\xi) + \lambda y(\xi) = f(\xi) \ (0 \le \xi \le T), \\ y(0) = v_0, y'(0) = v_1 \end{cases} \tag{2.1}$$

where $f(\xi) = f(\xi, x)$ is given abstract function and $y(\xi) = y(\xi, x)$ is an abstract function to be determined. In equation (2.1), P is a positive definite operator with the property of self-adjointness and has the following definition; $P^x = P \ge \delta I$, $\delta > 0$ and

$$P^x y(x) = -y_{xx} + \delta y(x) \tag{2.2}$$

with the domain

$$\Omega(P^x) = \left\{ y(x) : y, y_x, y_{xx} \in L_2[0, l], y(0) = y(l), y'(0) = y'(l) \right\}.$$

The function $y(\xi)$ is considered to be a solution to the problem (2.1) if it is twice continuously differentiable, $y(\xi) \in \Omega(P)$ and $Py(\xi)$ is continuous for all $\xi \in [0, T]$. In addition $y(\xi)$ satisfies the equation (2.1) and the given initial conditions.

It is obvious that the fractional order telegraph equation's problem (2.1) has a unique solution provided by the formula

$$\begin{aligned} y(\xi) \ = \ & (\lambda + P)^{-1} \Bigg[\left(\frac{\beta \sin \beta\pi}{\pi} \xi^{-\beta} + \frac{\alpha \sin \alpha\pi}{\pi} \xi^{-\alpha}\right) y(0) + \\ & f(t) + \frac{\beta \sin \beta\pi}{(1-\beta)\pi} \xi^{1-\beta} y'(0) - \frac{\beta^2 \sin \beta\pi}{\pi} \int_0^\xi (\xi - z)^{-1-\beta} y(z) dz \\ & - \frac{\alpha^2 \sin \beta\pi}{\pi} \int_0^\xi (\xi - z)^{-1-\alpha} y(z) dz \Bigg]. \end{aligned} \tag{2.3}$$

Using the definition (1.2) and partial integration, the formula (2.3) can be obtained easily. Here, $\frac{\pi}{\sin \beta\pi} = \beta \Gamma(1 - \beta)$.

3. Constructed finite difference schemes and stability estimates

In this section, we build both first order finite difference scheme (FOFDS) and second order finite difference scheme (SOFDS) for the problem (1.2) and give their stability estimate theorems. The boundary conditions are incorporated directly into the finite difference scheme at each time level. In particular, the boundary values are imposed explicitly at the boundary grid points and are used to update the solution at the interior points. These prescribed boundary values ensure that the numerical solution satisfies the given physical constraints throughout the computational domain. Consequently, at every time step, the scheme is applied only to the interior nodes while the boundary nodes are updated according to the given boundary conditions. For the numerical solution of the problem (2.1) to approximate in ξ, we give the FOFDS

$$\begin{cases} \frac{\tau^{-\beta}}{\Gamma(3-\beta)}\sum\limits_{j=0}^{k-1} w_j^{(\beta)}(y_{k-j+1}-2y_{k-j}+y_{k-j-1}) + \frac{\tau^{-\alpha}}{\Gamma(2-\alpha)}\sum\limits_{j=0}^{k} w_j^{(\alpha)}(y_{k-j+1}-y_{k-j}) + Py_k + \lambda y_k = f_k, \\ f_k = f(\xi_k), 1 \le k \le N-1, N\tau = T, \\ y_0 = v_0, \frac{m_1+m_2}{m_1}\frac{y_1-y_0}{\tau} + \tau^{-1}\left(P+\lambda I\right) y_0 = v_1 \end{cases} \tag{3.1}$$

where $m_1 = \frac{\tau^{-\beta}}{\Gamma(3-\beta)}$ and $m_2 = \frac{\tau^{-\alpha}}{\Gamma(2-\alpha)}$.

For the numerical solution of the problem (2.1) to approximate in ξ, we give the SOFDS

$$\begin{cases} \frac{\tau^{-\beta}}{\Gamma(3-\beta)}\sum\limits_{j=0}^{k-1} w_j^{(\beta)}(y_{k-j+1}-2y_{k-j}+y_{k-j-1}) + \frac{\tau^{-\alpha}}{\Gamma(2-\alpha)}\sum\limits_{j=0}^{k} w_j^{(\alpha)}(y_{k-j+1}-y_{k-j}) \\ +\frac{P}{2}(y_{k+1}+y_{k-1}) + \frac{\lambda}{2}\left(y_{k+1}+y_{k-1}\right) = f_k, \\ f_k = f(\xi_k), 1 \le k \le N-1, \\ y_0 = v_0, \frac{y_1-y_0}{\tau} = v_1 + \frac{\tau}{2}\frac{y_2-2y_1+y_0}{\tau^2},\ f_0 = f(0), \end{cases} \tag{3.2}$$

where, $w_j^{(\beta)} = (j+1)^{2-\beta} - j^{2-\beta}$ and $w_j^{(\alpha)} = (j+1)^{1-\alpha} - j^{1-\alpha}$.

The formula (3.1) can be rewritten as follows

$$\begin{cases} m_1 y_{k-1} - \left(2m_1+m_2-\lambda-P\right) y_k + \left(m_1+m_2\right) y_{k+1} \\ = f_k - \frac{\tau^{-\beta}}{\Gamma(3-\beta)}\sum\limits_{j=1}^{k-1} w_j^{(\beta)}(y_{k-j+1}-2y_{k-j}+y_{k-j-1}) \\ -\frac{\tau^{-\alpha}}{\Gamma(2-\alpha)}\sum\limits_{j=1}^{k} w_j^{(\alpha)}(y_{k-j+1}-y_{k-j}) = F_k, 1 \le k \le N-1, \\ y_0 = v_0, y_1 = (1-\frac{\lambda+P}{m_1+m_2})v_0 + \frac{1}{m_1+m_2}\tau v_1. \end{cases} \tag{3.3}$$

For the stability estimates formula (3.3), we will present the following theorem.

Theorem 3.1. *Suppose that $v_0 \in \Omega(P)$, $v_1 \in \Omega(P)$. Below stability estimate inequalties are satisfied for the first order difference scheme (3.3)*

$$\|y_1\|_H \le K(\alpha,\beta)\left\{\tau \parallel v_1 \parallel_H + \parallel v_0 \parallel_H\right\}$$

$$\max_{1\le k\le N}\|y_k\|_H \le K\left\{\max_{1\le k\le N-1}\|f_k\|_H + \parallel v_1 \parallel_H + \parallel v_0 \parallel_H\right\}. \tag{3.4}$$

Theorem 3.1 may be readily proven by employing

$$y_{k+1} = \tau\frac{2m_1+m_2-\lambda-P}{m_1+m_2}y_k - \frac{m_1}{m_1+m_2}y_{k-1} + \frac{1}{m_1+m_2}F_k.$$

For the second order, the formula (3.2) can be rewritten as follows

$$\begin{cases} (\frac{P}{2}+\frac{\lambda}{2}+m_1)y_{k-1}-(2m_1+m_2)\,y_k+\left(m_1+m_2+\frac{P}{2}+\frac{\lambda}{2}\right)y_{k+1} \\ =f_k-m_2\sum\limits_{j=1}^{k-1}w_j^{(\beta)}(y_{k-j+1}-2y_{k-j}+y_{k-j-1}) \\ -m_1\sum\limits_{j=1}^{k}w_j^{(\alpha)}(y_{k-j+1}-y_{k-j})=F_k, 1\leq k\leq N-1, \\ y_0=v_0,(m_1+m_2+\frac{\lambda+P}{2})\frac{y_1-y_0}{\tau}=(m_1-\frac{\lambda+P}{2})\tau v_1+f_0 \\ +(\frac{\lambda+P}{2}+m_1)\frac{\tau}{2}\frac{y_2-2y_1+y_0}{\tau^2}. \end{cases} \tag{3.5}$$

For the stability estimates formula (3.5), we will present the following theorem.

Theorem 3.2. *Suppose that $v_0\in\Omega(P),\ v_1\in\Omega(P)$. Below stability estimate inequalty is satisfied for the second order difference scheme (3.5)*

$$\max_{1\leq k\leq N}\|y_k\|_H\leq K(\alpha,\beta)\left\{\|f_k\|_H+\parallel v_1\parallel_H+\tau\parallel v_0\parallel_H\right\}. \tag{3.6}$$

Proof of the Theorem 3.2 can be easily done by using

$$y_{k+1}=\frac{2m_1+m_2}{m_1+m_2+\frac{\lambda+P}{2}}y_k-\tau\frac{m_1+\frac{\lambda+P}{2}}{m_1+m_2+\frac{\lambda+P}{2}}y_{k-1}+\frac{1}{m_1+m_2+\frac{\lambda+P}{2}}F_k.$$

4. Numerical Applications

We offer a numerical example for comparison and testing the first and second order accuracy of the Caputo time fractional order and classic integer order telegraph equation. To numerically calculate the solution of the problem (1.2), we take the grid space defined as $S_{\tau,h}=[0,T]_\tau\times[0,l]_h$. We use the same notation in [26] and take

$${}_0^C D_\xi^\beta y(\xi,x)\approx\frac{\tau^{-\beta}}{\Gamma(3-\beta)}\sum_{j=0}^{k-1}w_j^{(\beta)}(y_n^{k-j+1}-2y_n^{k-j}+y_n^{k-j-1}), \tag{4.1}$$

$${}_0^C D_\xi^\alpha y(\xi,x)\approx\frac{\tau^{-\alpha}}{\Gamma(2-\alpha)}\sum_{j=0}^{k}w_j^{(\alpha)}(y_n^{k-j+1}-y_n^{k-j}). \tag{4.2}$$

Using Taylor series method, we can obtain first order difference scheme in x

$$y_{xx}(\xi_k,x_n)\approx\frac{y_{n+1}^k-2y_n^k+y_{n-1}^k}{h^2}, \tag{4.3}$$

and second order difference scheme

$$y_{xx}(\xi_k,x_n)\approx\frac{1}{2}\frac{y_{n+1}^{k+1}-2y_n^{k+1}+y_{n-1}^{k+1}}{h^2}+\frac{1}{2}\frac{y_{n+1}^{k-1}-2y_n^{k-1}+y_{n-1}^{k-1}}{h^2}. \tag{4.4}$$

Using the formulas (4.1), (4.2) and (4.3), we discritize the problem (1.2) and obtain the following FOFDS

$$\begin{cases} \frac{\tau^{-\beta}}{\Gamma(3-\beta)}\sum_{j=0}^{k-1} w_j^{(\beta)}(y_n^{k-j+1}-2y_n^{k-j}+y_n^{k-j-1})+\frac{\tau^{-\alpha}}{\Gamma(3-\alpha)}\sum_{j=0}^{k} w_j^{(\alpha)}(y_n^{k-j+1}-y_n^{k-j})+y_n^k-\frac{y_{n+1}^k-2y_n^k+y_{n-1}^k}{h^2}=f_n^k, \\ x_n=nh, \xi_k=k\tau, 1\le k\le N-1, 1\le n\le M-1, \\ y_n^0=v_0(x_n), \frac{y_n^1-y_n^0}{\tau}=v_1(x_n),\ 0\le n\le M, \\ y_0^k=y_M^k=0,\ 0\le k\le N. \end{cases} \tag{4.5}$$

Using the formula (4.1), (4.2) and (4.4), we discritize the problem (1.2) and obtain the following SOFDS

$$\begin{cases} \frac{\tau^{-\beta}}{\Gamma(3-\beta)}\sum_{j=0}^{k-1} w_j^{(\beta)}(y_n^{k-j+1}-2y_n^{k-j}+y_n^{k-j-1})+\frac{\tau^{-\alpha}}{\Gamma(3-\alpha)}\sum_{j=0}^{k-1} w_j^{(\alpha)}(y_n^{k-j+1}-y_n^{k-j})-\frac{1}{2}\frac{y_{n+1}^{k+1}-2y_n^{k+1}+y_{n-1}^{k+1}}{h^2} \\ -\frac{1}{2}\frac{y_{n+1}^{k-1}-2y_n^{k-1}+y_{n-1}^{k-1}}{h^2}+\frac{1}{2}\left(y_n^{k+1}+y_n^{k-1}\right)=f_n^k, \\ x_n=nh, \xi_k=k\tau, 1\le k\le N-1,\ 1\le n\le M-1, \\ y_n^0=v_0(x_n), x_n=nh, \\ \frac{y_n^1-y_n^0}{\tau}=v_1(x_n)+\frac{\tau}{2}\frac{y_n^2-2y_n^1+y_n^0}{\tau^2},\ 0\le n\le M, \\ y_0^k=y_M^k=0,\ 0\le k\le N. \end{cases} \tag{4.6}$$

Example 4.1. Let's consider the following example equation,

$$\begin{cases} {}_0^CD_\xi^\beta y(\xi,x)+{}_0^C D_\xi^\alpha y(\xi,x)+\lambda y(\xi,x)=y_{xx}(\xi,x)+f(\xi,x), \\ f(\xi,x)=(6\frac{\xi^{3-\beta}}{\Gamma(4-\beta)}+6\frac{t^{3-\alpha}}{\Gamma(4-\alpha)}+(1+\pi^2)(\xi^3+1))\sin(\pi x), 0<\xi<1,\ 0<x<1, \\ y(0,x)=\sin(\pi x),\ y_\xi(0,x)=0,\ 0\le x\le 1, \\ y(\xi,0)=y(\xi,l)=0,\ 0\le\xi\le 1, \\ \lambda=1, 1<\beta\le 2,\ 0<\alpha\le 1. \end{cases} \tag{4.7}$$

Using the Laplace transform method, the analytical solution of the problem (4.7) can be easily obtained as

$$y(\xi,x)=(\xi^3+1)\sin\pi x.$$

To solve the difference equations (4.5) and (4.6), we use modified Gauss elimination method. Therefore, for $j=M-1,...,2,1$ the matrix solution is:

$$y_j=\eta_{j+1}y_{j+1}+\theta_{j+1},\ y_M=0.$$

Here, η_j is a square matrice with size $(N+1)\times(N+1)$, and θ_j is a column matrices with size $(N+1)\times 1$. They are defined as

$$\eta_{j+1}=-(B+C\eta_j)^{-1}A,$$
$$\theta_{j+1}=(B+C\eta_j)^{-1}(D\phi-C\theta_j),\ \ j=1,2,...,M-1.$$

Table 1 and 2 are constructed for the approximate solutions for N and M with $N^2 = M$ (or $h^2 = \tau$) and $\alpha = 0.5$, $\beta = 1.5$. The choice of the time step size τ and the spatial grid size h plays a crucial role in the accuracy and stability of the numerical scheme. In this study, these parameters are selected sufficiently small to ensure convergence of the proposed method and to capture the behavior of the solution with high accuracy.

In general, decreasing the values of τ and h improves the accuracy of the numerical solution; however, it increases the computational cost. On the other hand, larger values reduce the computational effort but may lead to a loss of accuracy and possible instability. Therefore, a suitable balance between computational efficiency and accuracy is maintained throughout the simulations.

The numerical experiments are carried out using fixed values of τ and h that satisfy the stability requirements of the method, and convergence of the scheme is verified through the obtained results. For different grid points of N, M and by using the following formula, we compute the errors between exact and numerical solution.

$$\varepsilon_N^M = \max_{1\leq k\leq N-1, 1\leq n\leq M-1} \left| y(\xi_k, x_n) - y_n^k \right|,$$

where y_n^k represents the numerical solution at (ξ_k, x_n) and the errors are recorded in Table 1 and 2. Also plot of the exact solution is given in Figure 1.

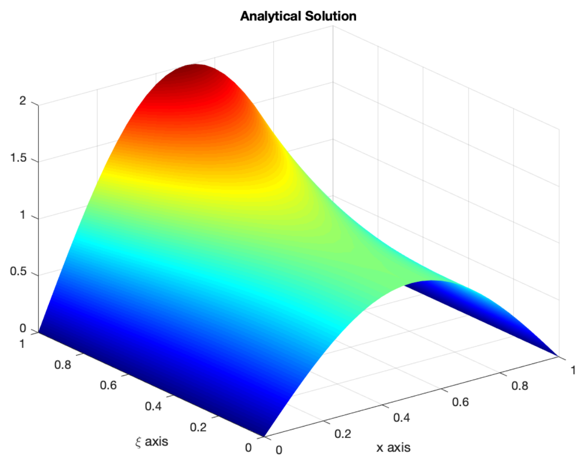

Figure 1: Graph of the analytical solution of the problem (4.7), where N=900 and M=30.

We give Table 1 and Figure 2,3,4,5 to present a comparison of the fractional order case with integer order case for the first order accuracy of the problem (4.7) using finite difference method.

Table 1: **Error Calculation for first order difference scheme** (4.5)

	First order accuracy (ε_N^M)	
N, M	$\alpha = 0.5, \beta = 1.5$	$\alpha = 1, \beta = 2$
$N = 25, M = 5$	0.12286	0.16761
$N = 100, M = 10$	0.030783	0.042811
$N = 400, M = 20$	0.0075601	0.010623
$N = 900, M = 30$	0.003342	0.0047149
$N = 1600, M = 40$	0.001875	0.0026509
$N = 2500, M = 50$	0.0011982	0.0016962

Table 1 shows that the fractional order case outperforms the standard integer order case in terms of absolute errors. We provide approximate solutions for fractional and integer order equations (1.2) utilizing first-order finite difference formulas (4.5).

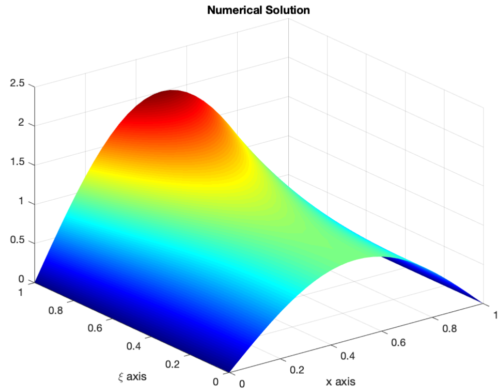

Figure 2: Set N=900, M=30, $\alpha = 0.5, \beta = 1.5$. Approximate solution for the fractional order case of the problem (4.7).

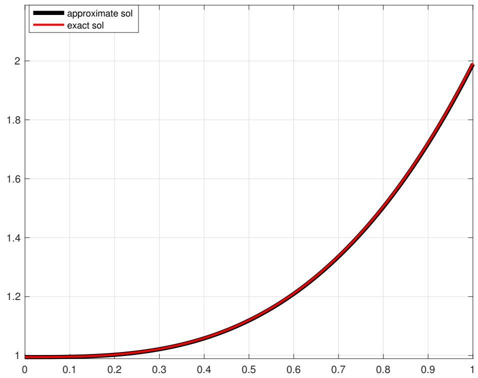

Figure 3: Shows exact and approximate solution for the fractional order case of the problem (4.7) are fitting together, where N=900, M=30, $\alpha = 0.5, \beta = 1.5$.

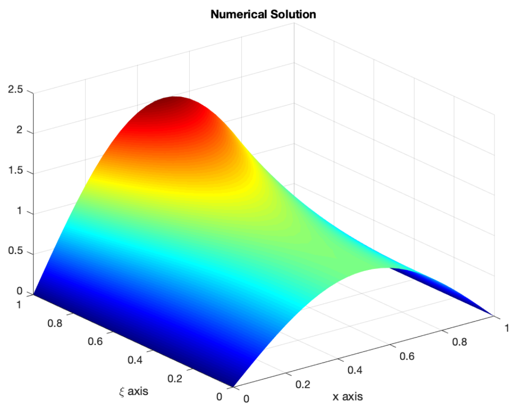

Figure 4: Approximate solution for the integer order case of the problem (4.7), where N=900, M=30, $\alpha = 1, \beta = 2$.

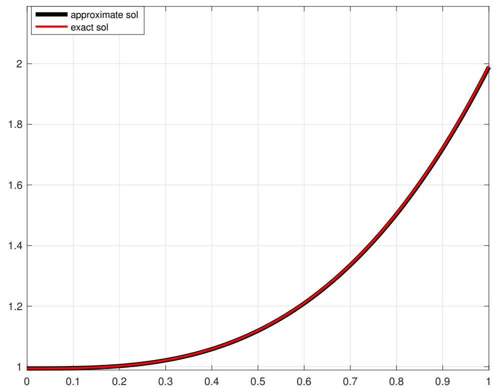

Figure 5: Shows exact and approximate solution for the fractional order case of the problem (4.7) are fitting together, where N=900, M=30, $\alpha = 1, \beta = 2$.

Also in Figure 6, the 2D residual heatmap indicates that the numerical scheme satisfies the governing equation with high precision, as the residual values are uniformly close to zero throughout the domain. This further validates the robustness and reliability of the proposed method.

Next, we give Table 2 and Figure 7,8,9,10 to present a comparison of the fractional order case with integer order case for the second order accuracy of the problem (4.7) using finite difference method.

Table 2 shows that the fractional order case outperforms the standard integer order case in terms of absolute errors. We provide approximate solutions to the fractional and integer order equations (1.2) utilizing second order finite difference formulas (4.6).

In Figure 11 the residual distribution is illustrated using a 2D heatmap via the imagesc function. The results indicate that the residual values remain very small throughout the computational domain, confirming the accuracy of the proposed method.

From Table 1, 2 and all figures, computer simulations confirm that both difference schemes are efficient,

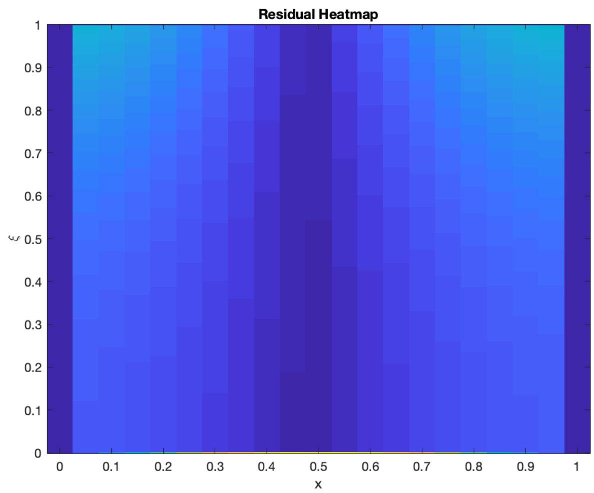

Figure 6: Graph of the residual heatmap of the problem (4.7), where N=400 and M=20, $\alpha = 0.5, \beta = 1.5$.

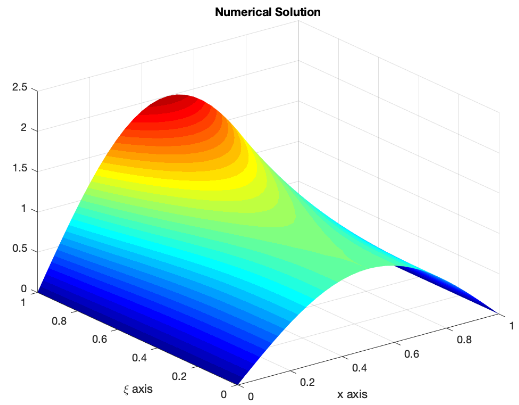

Figure 7: Set N=900, M=30, $\alpha = 0.5, \beta = 1.5$. Approximate solution for the fractional order case of the problem (4.7).

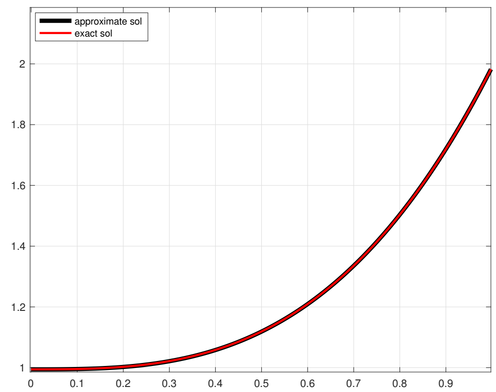

Figure 8: Shows exact and approximate solution for the fractional order case of the problem (4.7) are fitting together, where N=900, M=30, $\alpha = 0.5, \beta = 1.5$.

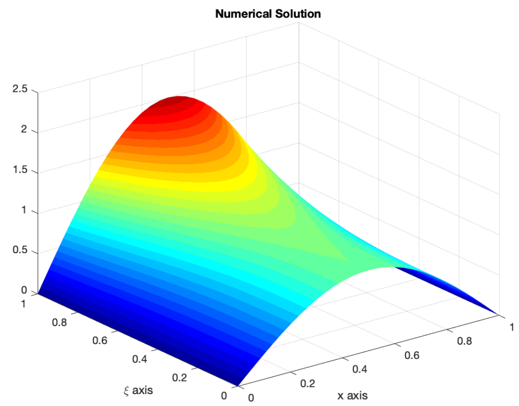

Figure 9: Approximate solution for the integer order case of the problem (4.7), where N=900, M=30, $\alpha = 1, \beta = 2$.

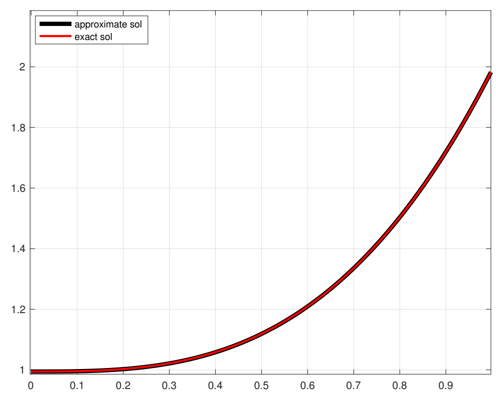

Figure 10: Shows exact and approximate solution for the fractional order case of the problem (4.7) are fitting together, where N=900, M=30, $\alpha = 1, \beta = 2$.

Table 2: **Error Calculation for second order difference scheme** (4.6)

	Second order accuracy (ε_N^M)	
N, M	$\alpha = 0.5, \beta = 1.5$	$\alpha = 1, \beta = 2$
$N = 25, M = 5$	0.018495	0.04356
$N = 100, M = 10$	0.0042047	0.012148
$N = 400, M = 20$	0.0009338	0.0030817
$N = 900, M = 30$	0.00039641	0.0013734
$N = 1600, M = 40$	0.00021764	0.00077325
$N = 2500, M = 50$	0.00013722	0.0004951

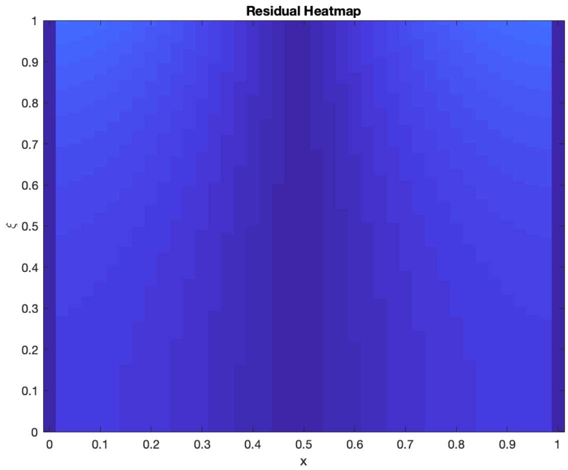

Figure 11: Graph of the residual heatmap of the problem (4.7), where N=1600 and M=40, $\alpha = 0.5, \beta = 1.5$.

with the SOFDS providing greater accuracy than the FOFDS. To enhance the clarity of the numerical results, the figures are annotated to highlight the key features of the solutions. In particular, the differences between the fractional-order and integer-order cases are emphasized in the graphical representations. These annotations help to clearly illustrate the effect of the fractional parameters on the solution behavior.

5. Conclusion

In this study, we analyzed the time-fractional telegraph equation using the Caputo derivative and developed both first-order and second-order finite difference schemes to approximate its solution. Rigorous stability analyses were performed for each scheme, confirming their reliability under appropriate conditions. A comprehensive numerical experiment was conducted to compare the accuracy of fractional-order and classical integer-order models using a test problem with a known exact solution.

The results clearly indicate that the fractional-order model provides a more accurate approximation of the solution than the classical model, particularly when using the second-order finite difference scheme. Furthermore, the second-order method consistently outperforms the first-order method in terms of precision, making it a more suitable choice for solving such fractional partial differential equations. The close agreement between the numerical and analytical solutions, as illustrated in the figures, validates the effectiveness of the proposed methods.

These findings highlight the advantages of incorporating fractional calculus into mathematical modeling and demonstrate the potential of the proposed finite difference schemes for solving more complex real-world problems governed by fractional dynamics.

The proposed numerical approach can be extended to a variety of fractional-order models arising in physics and engineering, such as diffusion, wave propagation, and financial models. As a future direction, the method may be applied to higher-dimensional problems and more complex nonlinear fractional systems. In addition, the development of more efficient and adaptive schemes could further improve the accuracy and computational performance of the approach.

References

[1] A. Akgül and M. Modanli. Crank-nicholson difference method and reproducing kernel function for third order fractional differential equations in the sense of atangana-baleanu caputo derivative. *Chaos, Solitons & Fractals*, 127:10–16, 2019. 1

[2] A. Ashyralyev and M. Modanli. An operator method for telegraph partial differential and difference equations. *Boundary Value Problems*, 2015(1):1–17, 2015. 2

[3] A. Atangana, A. Akgül, and K. M. Owolabi. Analysis of fractal fractional differential equations. *Alexandria Engineering Journal*, 59(3):1117–1134, 2020. 1

[4] D. Baleanu, S. S. Sajjadi, A. Jajarmi, O. Defterli, and J. H. Asad. The fractional dynamics of a linear triatomic molecule. *Romanian Reports in Physics*, 73(1):105, 2021. 1

[5] W. Beghami, B. Maayah, S. Bushnaq, and O. Abu Arqub. The laplace optimized decomposition method for solving systems of partial differential equations of fractional order. *International Journal of Applied and Computational Mathematics*, 8(2):52, 2022. 1

[6] M. Fanwei. A new approach for solving fractional partial differential equation. *Journal of Applied Mathematics*, 2013:5, 2013. 1

[7] R. Gnitchogna and A. Atangana. New two step laplace adam-bashforth method for integer and noninteger order partial differential equations. *Numerical Methods for Partial Differential Equations*, 34(5):1739–1758, 2018. 1

[8] Z. Hammouch and T. Mekkaoui. A laplace-variational iteration method for solving the homogeneous smoluchowski coagulation equation. *Applied Mathematical Sciences*, 6(18):879–886, 2012. 1

[9] I. U. Haq, N. Ali, S. Ahmad, and T. Akram. A hybrid interpolation method for fractional pdes and its applications to fractional diffusion and buckmaster equations. *Mathematical Problems in Engineering*, 2022, 2022. 1

[10] M. S. Hashmi, U. Aslam, J. Singh, and K. S. Nisar. An efficient numerical scheme for fractional model of telegraph equation. *Alexandria Engineering Journal*, 61(8):6383–6393, 2022. 1

[11] S. Herdem and M. S. Mamis. Computation of corona effects in transmission lines using state-space techniques. *Computers and Electrical Engineering*, 29(5):603–611, 2003. 1

[12] K. Hosseini, M. Samavat, M. Mirzazadeh, W. X. Ma, and Z. Hammouch. A new-dimensional hirota bilinear equation: its bäcklund transformation and rational-type solutions. *Regular and Chaotic Dynamics*, 25(4):383–391, 2020. 1

[13] A. Houwe, J. Sabi'u, Z. Hammouch, and S. Y. Doka. Solitary pulses of a conformable nonlinear differential equation governing wave propagation in low-pass electrical transmission line. *Physica Scripta*, 95(4):045203, 2020. 1

[14] J. A. Hudson. *The Excitation and Propagation of Elastic Waves*. Cambridge University Press, Cambridge, UK, 1980. 1

[15] H. Khan, R. Shah, P. Kumam, D. Baleanu, and M. Arif. Laplace decomposition for solving nonlinear system of fractional order partial differential equations. *Advances in Difference Equations*, 2020(1), 2020. 1

[16] P. Kumar, V. S. Erturk, H. Abboubakar, and K. S. Nisar. Prediction studies of the epidemic peak of coronavirus disease in brazil via new generalised caputo type fractional derivatives. *Alexandria Engineering Journal*, 60(3):3189–3204, 2021. 1

[17] E. Loghman, A. Kamali, F. Bakhtiari-Nejad, M. Abbaszadeh, and M. Amabili. On the combined shooting-pseudo-arclength method for finding frequency response of nonlinear fractional-order differential equations. *Journal of Sound and Vibration*, 516:116521, 2022. 1

[18] M. S. Mamis and M. Koksal. Remark on the lumped parameter modeling of transmission lines. *Electric Machines and Power Systems*, 28(6):565–575, 2000. 1

[19] M. Modanli and A. Akgül. Numerical solution of fractional telegraph differential equations by theta-method. *European Physical Journal Special Topics*, 226(16–18):3693–3703, 2017. 1

[20] M. Modanli and F. Ozbag. Stability of finite difference schemes for two-space dimensional telegraph equation. *Pramana*, 96(4):228, 2022. 1

[21] M. Naeem, O. F. Azhar, A. M. Zidan, K. Nonlaopon, and R. Shah. Numerical analysis of fractional-order parabolic equations via elzaki transform. *Journal of Function Spaces*, 2021:1–10, 2021. 1

[22] Z. A. Noor, I. Talib, and M. B. Riaz. Computational advancements in spectral methods for solving fractional-order differential equations. *Fractals*, 33(6):1–17, 2025. 1

[23] W. M. Osman, T. M. Elzaki, and N. A. A. Siddig. Modified double conformable laplace transform and singular fractional pseudohyperbolic and pseudo-parabolic equations. *Journal of King Saud University-Science*, 33(3):101378, 2021. 1

[24] F. Ozbag and E. Karafilikoglu. Investigation of traveling wave solutions of the cubic nonlinear space-time fractional telegraph equation. *Physica Scripta*, 101(11):115206, 2026. 1

[25] O. Ozkan and A. Kurt. A new method for solving fractional partial differential equations. *Journal of Analysis*, 28(2):489–502, 2020. 1

[26] I. Podlubny. Fractional order systems and pi\lambda/d\mu-controllers. *IEEE Transactions on Automatic Control*, 44(1):208–214, 1999. 4

[27] S. Rashid, Z. Hammouch, D. Baleanu, and Y. M. Chu. New generalizations in the sense of the weighted non-singular fractional integral operator. *Fractals*, 28(8):2040003, 2020. 1

[28] J. Singh, D. Kumar, and A. Kilicman. Numerical solutions of nonlinear fractional partial differential equations arising in spatial diffusion of biological populations. *Abstract and Applied Analysis*, 2014:1–12, 2014. 1

[29] I. Talib, T. Abdeljawad, and M. A. Alqudah. A high-precision spectral method for solving bagley–torvik equations. *Computers and Applied Mathematics*, 44:412, 2025. 1

[30] M. F. Uddin, M. G. Hafez, Z. Hammouch, H. Rezazadeh, and D. Baleanu. Traveling wave with beta derivative spatial-temporal evolution for describing the nonlinear directional couplers with metamaterials via two distinct methods. *Alexandria Engineering Journal*, 60(1):1055–1065, 2021. 1

[31] J. L. Wu. A wavelet operational method for solving fractional partial differential equations numerically. *Applied Mathematics and Computation*, 214(1):31–40, 2009. 1

[32] L. Zada, R. Nawaz, S. Ahsan, K. S. Nisar, and D. Baleanu. New iterative approach for the solutions of fractional order inhomogeneous partial differential equations. *AIMS Mathematics*, 2020. 1

[33] D. Zaidi, I. Talib, M. B. Riaz, and M. N. Alam. Extending spectral methods to solve time fractional-order bloch equations using generalized laguerre polynomials. *Partial Differential Equations in Applied Mathematics*, 13:101049, 2025. 1

[34] M. Zayernouri, M. Ainsworth, and G. E. Karniadakis. A unified petrov–galerkin spectral method for fractional pdes. *Computer Methods in Applied Mechanics and Engineering*, 283:1545–1569, 2015. 1